



THE UNIVERSITY *of* EDINBURGH

Edinburgh Research Explorer

G -type antiferromagnetic order in the metallic oxide $\text{LaCu}_3\text{Cr}_4\text{O}_{12}$

Citation for published version:

Saito, T, Zhang, S, Khalyavin, D, Manuel, P, Attfield, JP & Shimakawa, Y 2017, 'G -type antiferromagnetic order in the metallic oxide $\text{LaCu}_3\text{Cr}_4\text{O}_{12}$ ', *Physical review B*, vol. 95, no. 4, 041109.
<https://doi.org/10.1103/PhysRevB.95.041109>

Digital Object Identifier (DOI):

[10.1103/PhysRevB.95.041109](https://doi.org/10.1103/PhysRevB.95.041109)

Link:

[Link to publication record in Edinburgh Research Explorer](#)

Document Version:

Peer reviewed version

Published In:

Physical review B

General rights

Copyright for the publications made accessible via the Edinburgh Research Explorer is retained by the author(s) and / or other copyright owners and it is a condition of accessing these publications that users recognise and abide by the legal requirements associated with these rights.

Take down policy

The University of Edinburgh has made every reasonable effort to ensure that Edinburgh Research Explorer content complies with UK legislation. If you believe that the public display of this file breaches copyright please contact openaccess@ed.ac.uk providing details, and we will remove access to the work immediately and investigate your claim.



Supplementary Material for “G-type antiferromagnetic order in metallic oxide $\text{LaCu}_3\text{Cr}_4\text{O}_{12}$ ”

Takashi Saito (齊藤高志),^{1,*} Shoubao Zhang (張守寶),¹ Dmitry Khalyavin², Pascal Manuel², J. Paul Attfield,³ and Yuichi Shimakawa (島川祐一)^{1,4}

¹Institute for Chemical Research, Kyoto University, Uji, Kyoto 611-0011, Japan

²ISIS, Rutherford Appleton Laboratory, Harwell Oxford, Didcot OX11 0QX, United Kingdom

³Centre for Science at Extreme Conditions and School of Chemistry, University of Edinburgh, Mayfield Road, Edinburgh EH9 3JZ, United Kingdom

⁴Japan Science and Technology Agency, CREST, Uji, Kyoto 611-0011, Japan

Here we provide the results of the Rietveld analysis of the neutron powder diffraction (NPD) data of $\text{LaCu}_3\text{Cr}_4\text{O}_{12}$, details of the bond valence sum calculations, and the details of the calculated density of states (DOSs) of the lowest energy model.

The result of the fitting for the NPD data at 300 K is shown in Fig. S1. The refined structural parameters at 300 K are summarized in Table S-I, and the selected bond distances and bond angles at 300, 250, 200 and 5 K are summarized in Table S-II. The refined magnetic moments of the B-site Cr spins obtained with the temperature dependent NPD data are plotted in Fig. S2.

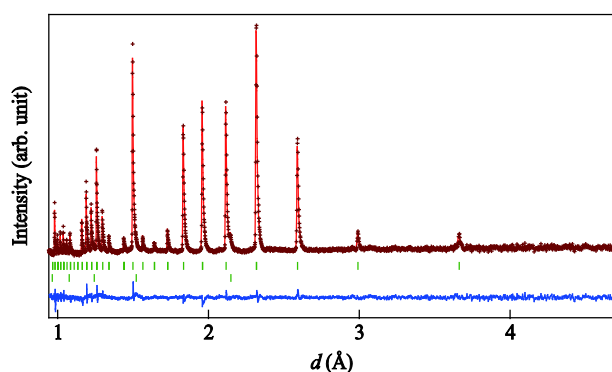


FIG. S1. Rietveld plot of the neutron powder diffraction pattern of $\text{LaCu}_3\text{Cr}_4\text{O}_{12}$ at 300 K. The observed (+) calculated (solid line) patterns are shown along with the difference between them (bottom). The ticks indicate the allowed Bragg reflections for $\text{LaCu}_3\text{Cr}_4\text{O}_{12}$ (above) and the vanadium container (below).

TABLE S-I. Results of the Rietveld refinement of the neutron powder diffraction data for $\text{LaCu}_3\text{Cr}_4\text{O}_{12}$ at 300 K. The Wyckoff positions in space group $Im\bar{3}$, coordinates, isotropic atomic displacement parameter B_{iso} , site occupancy, and lattice parameter are listed together with the reliability factors.

Atom	Wyckoff pos.	x	y	z	$B_{\text{iso}} (\text{\AA}^2)$	Occ.
La	$2a$	0	0	0	1.5(1)	1
Cu	$6b$	0	$\frac{1}{2}$	$\frac{1}{2}$	0.62(9)	1
Cr	$8c$	$\frac{1}{4}$	$\frac{1}{4}$	$\frac{1}{4}$	0.5(1)	1
O	$24g$	0	0.1786(2)	0.3055(2)	0.92(9)	1

$a = 7.3198(2) \text{ \AA}$
 $R_{\text{wp}} = 2.50 \text{ \%, } R_{\text{B}} = 4.08 \text{ \%$

TABLE S-II. Selected bond distances and bond angles of $\text{LaCu}_3\text{Cr}_4\text{O}_{12}$ at 300, 250, 200, and 5 K.

Temperature	300 K	250 K	200 K	5 K
Bond distances /Å				
La–O ($\times 12$)	2.590(2)	2.585(2)	2.589(1)	2.590(1)
Cu–O ($\times 4$)	1.933(2)	1.946(2)	1.9324(8)	1.917(1)
Cu–O ($\times 4$)	2.7498(8)	2.750(2)	2.750(1)	2.7506(5)
Cu–O ($\times 4$)	3.246(1)	3.234(2)	3.2448(9)	3.2557(7)
Cr–O ($\times 6$)	1.9460(5)	1.9422(7)	1.9454(4)	1.9484(9)
Bond angles /degree				
Cr–O–Cr	140.23(8)	140.89(3)	140.23(2)	139.47(6)
O–Cr–O	90.01(7)/89.99(7)	90.3(2)/89.7(2)	90.03(5)/89.97(6)	90.10(5)/89.90(5)
Cr–O–Cu	109.6(1)	109.24(8)	109.59(4)	109.97(5)

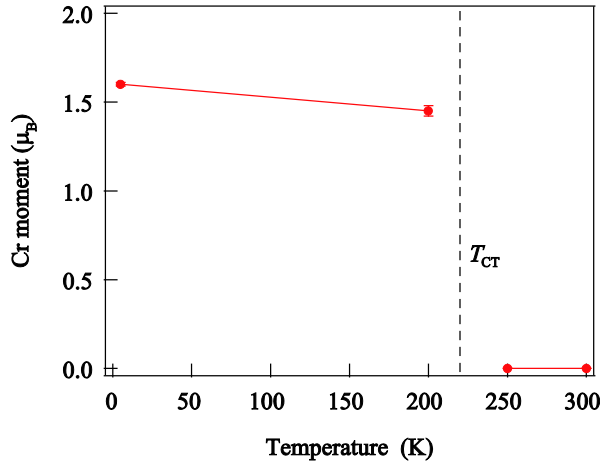


FIG. S2. Temperature dependence of the refined magnetic moment at Cr site obtained from the Rietveld analysis of the neutron powder diffraction data. Charge transfer transition temperature is shown by a broken line.

The results of the NPD structure analysis with the accurate bond distances r_i from the cation site to the coordinating oxygens enable the formal charges of the cations to be estimated using the bond valence sum method [1]. Bond valence sum (V_N) is given by the formula $V_N = \sum_i \exp[(r_N - r_i)/0.37]$, where r_N is the bond valence parameter for the metal in an assumed oxidation state N . The charges of the mixed valent Cu and Cr were estimated by interpolation between V_N values obtained for $\text{Cu}^{2+}/\text{Cu}^{3+}$ and $\text{Cr}^{3+}/\text{Cr}^{4+}$, using the formula $V_N = [L(V_H - V_L) - (H - L)V_L]/[(V_H - V_L) - (H - L)]$, where H and L are the higher and lower formal oxidation states [2]. As the r_4 for 6-fold coordinated $\text{Cr}^{4+}\text{--O}^{2-}$ bond in ref. 1 is not reliable, it was calculated using the previously reported bond distances of SrCrO_3 [3], CaCrO_3 [4] and CrO_2 [5,6]. r_4 was calculated for each reported structure assuming $V_4 = 4.00$ for Cr [7], and the averaged value of 1.756 was used in the present study. Bond valence sums of Cu and Cr were summed over 12 and 6 bonds, respectively. The interpolated charges were normalized to the total of +21 for the formal sum of the Cu and Cr charges per formula unit. The resulting charges are $\text{LaCu}^{2.47+}_3\text{Cr}^{3.39+}_4\text{O}_{12}$ at 300 K (corresponding to $\delta = 0.47$) and $\text{LaCu}^{2.59+}_3\text{Cr}^{3.31+}_4\text{O}_{12}$ ($\gamma = 0.41$) at 5 K. The estimated intersite charge transfer is $0.12e$ per Cu ion. The obtained results are consistent with the previously reported results obtained from the synchrotron X-ray diffraction data [7].

We also provide the results of the *ab initio* calculations. Total energy of a spin polarized model with nonmagnetic Cu and G-type AFM Cr spins was compared to those with a paramagnetic case with nonmagnetic Cu and Cr ions, and a ferrimagnetic case with antiferromagnetically coupled FM sublattices of Cu and Cr spins. Electron correlations are taken into account in the calculations. The results are summarized in Table S-III.

TABLE S-III. Total energy differences in spin polarized models.

(1) Standard calculation without U_{eff}

Model	nonmagnetic Cu & G-type AFM Cr	Paramagnetic: PM Cu & PM Cr	Ferrimagnetic: FM Cu & FM Cr	Ferromagnetic: FM Cu & FM Cr
Energy difference (eV)	-	+2.07	+0.16	converged to a ferrimagnetic model

(2) Calculation with $U_{\text{eff}} = 2$ eV for *B*-site Cr

Model	nonmagnetic Cu & G-type AFM Cr	Paramagnetic: PM Cu & PM Cr	Ferrimagnetic: FM Cu & FM Cr	Ferromagnetic: FM Cu & FM Cr
Energy difference (eV)	-	+4.80	+0.41	converged to a ferrimagnetic model

(3) Calculation with $U_{\text{eff}} = 2$ eV for *A'*-site Cu and $U_{\text{eff}} = 2$ eV for *B*-site Cr

Model	nonmagnetic Cu & G-type AFM Cr	Paramagnetic: PM Cu & PM Cr	Ferrimagnetic: FM Cu & FM Cr	Ferromagnetic: FM Cu & FM Cr
Energy difference (eV)	-	+4.83	+0.12	converged to a ferrimagnetic model

(4) Calculation with $U_{\text{eff}} = 4$ eV for *B*-site Cr

Model	nonmagnetic Cu & G-type AFM Cr	Paramagnetic: PM Cu & PM Cr	Ferrimagnetic: FM Cu & FM Cr	Ferromagnetic: FM Cu & FM Cr
Energy difference (eV)	-	+8.15	+0.55	converged to a ferrimagnetic model

Even when electron correlations were taken into account in the calculations, the spin polarized model with nonmagnetic Cu and G-type AFM Cr spins, which was confirmed by NPD magnetic structure analysis, was found to give the lowest total energy. Therefore, the discussion in the present study was based on the result with (1) standard calculation without U_{eff} .

The calculated total and partial DOSs of the experimentally obtained spin structure are shown in Fig. S3. The bands approaching the Fermi level (E_F) at the R point have rather linear k -dependences like a Dirac cone along the Γ –R direction, as shown in Fig. S4, although those above and below E_F rapidly bend back away from each other in the very vicinity of the R point. Magnetoresistance as reported for some Dirac electron systems was not observed for the present $\text{LaCu}_3\text{Cr}_4\text{O}_{12}$.

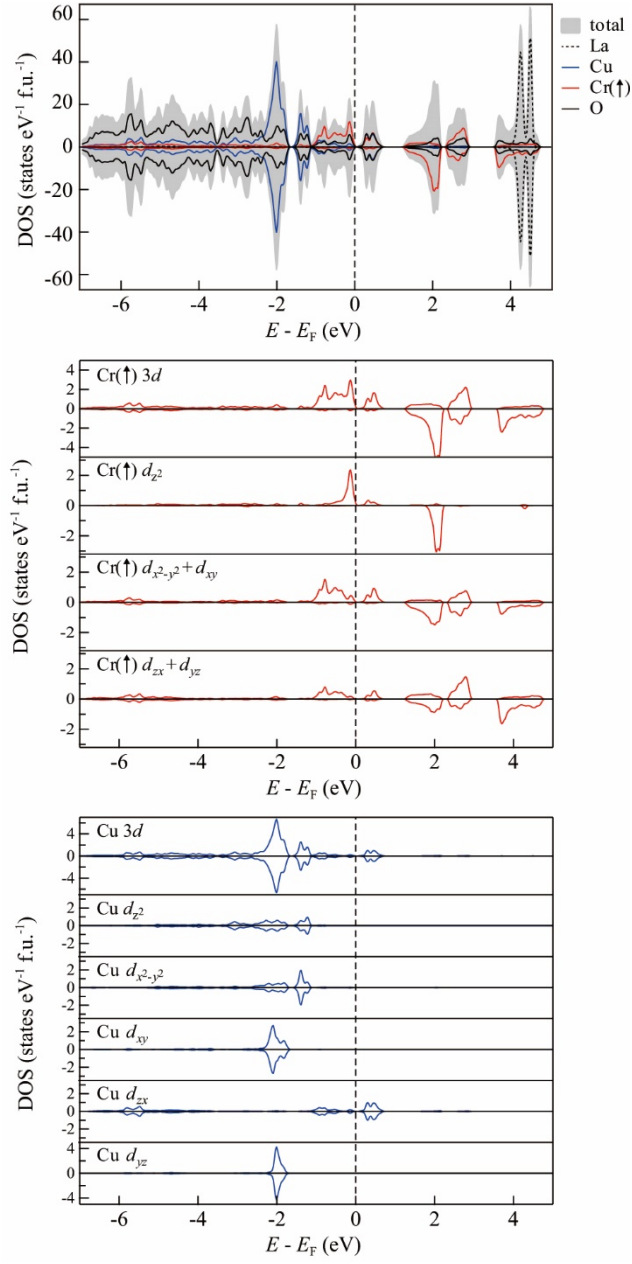


FIG. S3. Calculated total and partial DOSs for $\text{LaCu}_3\text{Cr}_4\text{O}_{12}$. E_F is the Fermi energy.

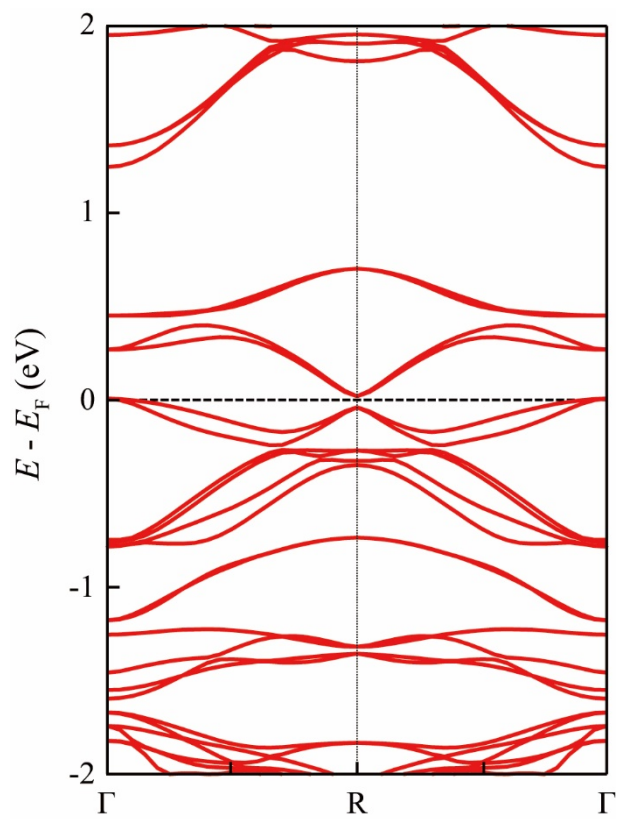


FIG. S4. The band structure along the Γ -R direction.

References

- [1] I. D. Brown and D. Altermatt, *Acta Crystallogr. Sect. B* **41**, 244 (1985).
- [2] J. P. Attfield, *Solid State Sciences* **8**, 861 (2006).
- [3] C. P. Khattak and D. E. Cox, *Mater. Res. Bull.* **12**, 463 (1977).
- [4] E. Castillo-Martinez, A. Durán, and M. Á. Alario-Franco, *J. Solid State Chem.* **181**, 895 (2008)
- [5] K. Siratori and S. Iida, *J. Phys. Soc. Jpn.* **15**, 2362 (1960).
- [6] G. Tirao, S. Ceppi, A. L. Cappelletti, and E. V. Pannunzio Miner, *J. Phys. Chem. Solids* **71**, 199 (2010).
- [7] S. Zhang, T. Saito, M. Mizumaki, and Y. Shimakawa, *Chem. Eur. J.* **20**, 9510 (2014).